

Raman and IR studies of surface metal oxide species on oxide supports: Supported metal oxide catalysts

Israel E. Wachs

Zettlemoyer Center for Surface Studies and Department of Chemical Engineering, Lehigh University, Bethlehem, PA 18015, USA

Abstract

Raman and infrared spectroscopy provide complementary information about the nature of the surface metal oxide species present in supported metal oxide catalysts. This paper reviews the type of fundamental information that is typically obtained in Raman and IR characterization studies of supported metal oxide catalysts. The molecular structures of the surface metal oxide species are reflected in the terminal $M=O$ and bridging $M-O-M$ vibrations. The location of the surface metal oxide species on the oxide supports is determined by directly monitoring the specific surface hydroxyls of the support that are being titrated. The surface coverage of the surface metal oxide species on the oxide supports can be quantitatively obtained since at monolayer coverage all the reactive surface hydroxyls are titrated and additional metal oxide results in the formation of crystalline metal oxide particles. The nature of surface Lewis and Brønsted acid sites present in supported metal oxide catalysts are determined by adsorbing basic probe molecules like pyridine. Information about the behavior of the surface metal oxide species during catalytic reactions are provided by in situ characterization studies. Such fundamental information is critical for the development of molecular structure–reactivity relationships for supported metal oxide catalysts. This paper will be limited to supported metal oxide catalysts containing group V–VII transition metal oxides (e.g., V, Nb, Cr, Mo, W and Re) on several different oxide supports (alumina, titania, zirconia, niobia and silica).

Keywords: Raman spectrometry; Infrared spectrometry; Supported metal oxide catalysts; Molecular structure; Surface chemistry

1. Introduction

Surface metal oxide species on oxide supports are typically formed when one metal oxide is deposited on a second metal oxide possessing a high surface area. For many oxide systems, the deposited metal oxide preferentially forms a two-dimensional surface metal oxide overlayer (surface metal oxide species) rather than a separate crystalline metal oxide phase or compound with the oxide support [1]. The preferential formation of the surface metal oxide species is thermodynamically driven in order to lower the surface free energy of the mixed oxide system.

The surface metal oxide species is usually the active catalytic component (rhenium oxide, chromium oxide, molybdenum oxide, tungsten oxide, vanadium oxide, etc.) on the high surface area oxide support (alumina, titania, zirconia, niobia, silica, etc.) in such supported metal oxide catalysts. Supported metal oxide catalysts find wide application in the petroleum, chemical and pollution control industries [2,3].

The characterization methods generally applicable to supported metal oxide catalysts have recently been reviewed [3]. Raman and infrared are complementary spectroscopies that are among the unique characterization techniques

that have provided fundamental molecular level information about the surface properties of supported metal oxide catalysts: molecular structure of the surface metal oxide species (ambient and in situ conditions), location of the surface metal oxide species, surface coverage of the metal oxide overlayer, distribution of surface Lewis and Brønsted acid sites as well as the structure of the active surface metal oxide species during catalytic reactions. The present paper will show the types of information usually reported in the literature for supported metal oxide catalysts from Raman and infrared spectroscopic characterization studies. The examples shown will primarily be taken from the author's publications in this area since it will allow comparison of Raman and IR data for the exact same samples and experimental conditions. The paper will also be limited to supported metal oxide catalysts involving the group V–VII transition metal oxides (oxides of Re, Cr, Mo, W, V and Nb) since much is known about these oxides and they constitute some of the most important catalytic systems [2]. Although this paper is not a review of the literature, a historical perspective of the significant contributions to this field during the past two decades is also included.

2. Raman and IR of oxide supports

Raman and infrared spectroscopy are complementary methods for the study of molecular vibrations. The intensities of IR absorption bands depend on the change of the dipole moment brought about by variations in the molecular geometry for the vibration concerned, while the intensities of Raman bands depend on the change of polarizability associated with the vibration [4]. Consequently, bonds possessing ionic character tend to give strong IR signals and bonds possessing covalent character tend to give strong Raman signals. The IR (700–1100 cm^{-1}) and Raman (100–1100 cm^{-1}) spectra of some typical oxide supports are presented in Figs. 1 and 2, respectively [5]. Alumina, titania and zirconia

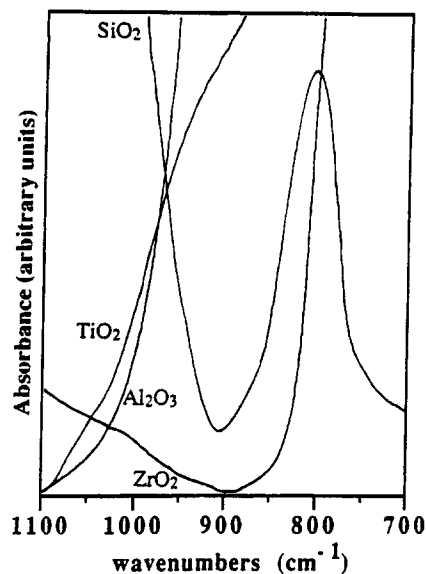


Fig. 1. Infrared spectra of oxide supports (dehydrated at 500°C).

possess strong IR absorptions due to the ionic character of their $M\text{--}O$ bonds below approximately 1000, 950 and 800 cm^{-1} , respectively; silica possesses strong IR absorptions above approximately 1000 and below 700 cm^{-1} as well as a strong absorption at 800 cm^{-1} due to the ionic character of the $\text{Si}\text{--}O$ bond. In contrast, these same oxide supports give rise to

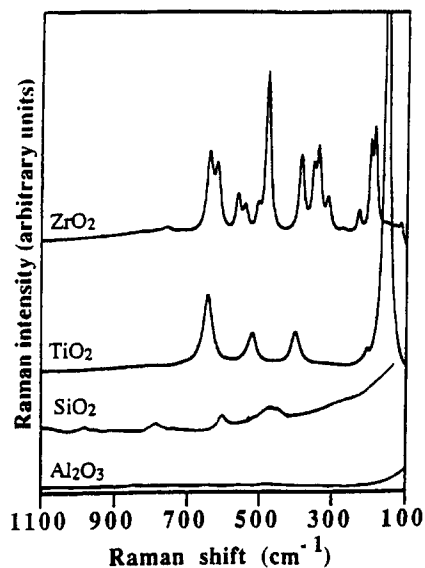


Fig. 2. Raman spectra of oxide supports (dehydrated at 500°C).

very weak Raman signals in the 700–1100 cm^{-1} region. Furthermore, the silica and alumina supports do not exhibit any Raman bands or only very weak ones in the 100–1100 cm^{-1} region due to the low polarizability of light atoms and the ionic character of the Al–O and Si–O bonds. The titania and zirconia supports do possess strong Raman bands below approximately 700 cm^{-1} because their M –O bonds do possess some covalent bonding character. The IR and Raman vibrational characteristics of the oxide supports have important implications for the detection of the vibrations of the surface metal oxide species which usually vibrate in the 100–1100 cm^{-1} region (see below). Thus, Raman spectroscopy is better suited than IR spectroscopy to detect the molecular vibrations of surface metal oxide species on oxide supports in the lower wavenumber region (location of M –O and M –O– M bonds) and both Raman and IR spectroscopy can generally provide complementary molecular vibrational information about the surface metal oxide species on oxide supports in the higher wavenumber region (location of M =O bonds).

The oxide supports generally terminate with M –OH bonds which are quite polar and give rise to strong IR bands in the 3000–4000 cm^{-1} region [6]. These surface hydroxyls give rise to weak Raman signals which can sometimes be detected for oxide supports such as titania and silica [7,8]. However, the superior surface hydroxyl signals observed with IR spectroscopy

has made this characterization technique the method of choice when investigating the surface hydroxyl chemistry of supported metal oxide catalysts.

3. Molecular structure of surface metal oxide species

3.1. Ambient conditions

Under ambient conditions, the supported metal oxide catalysts contain a thin film of water which hydrates the surface metal oxide species [9]. The M =O and M –O vibrations of the hydrated surface metal oxide species generally occur below 1000 cm^{-1} which usually makes it difficult to detect these vibrations with IR spectroscopy because of the strong IR absorption of the oxide supports in this region. For some systems, it is occasionally possible to at least detect the terminal M =O vibration in the 900–1000 cm^{-1} region if the support absorption is not too strong in this region (especially zirconia) and a high surface coverage of surface metal oxide species is present. In contrast, the Raman spectra of the hydrated surface metal oxide species are readily measured below 1000 cm^{-1} and the band positions for monolayer coverages on alumina are presented in Table 1. Comparison of the Raman bands of the hydrated surface metal oxide species on alumina with the corresponding aqueous metal oxide species re-

Table 1
Comparison of Raman bands (in cm^{-1}) of aqueous metal oxide species with ambient surface metal oxide species on alumina

	ReO_4^- (aq) [9,30]	$\text{Cr}_3\text{O}_{10}^{2-}$ (aq) [11]
aqueous solution	971, 916, 332	987, 956, 904, 844, 524, 378, 366, 214
monolayer on Al_2O_3 (ambient conditions)	982, 920, 332	—, 960, 896, 850, —, —, 362, 217
	$\text{Mo}_8\text{O}_{26}^{4-}$ (aq) [12]	$\text{V}_{10}\text{O}_{28}^{6-}$ (aq) [9]
aqueous solution	965, 925, 590, 370, 230	994, 970, 840, 600, 547, 458, 324, 251, 210, 185
monolayer on Al_2O_3 (ambient conditions)	958, 865, 555, 348, 216	995, 940, 820, 565, 500, —, 290, 250, —, 180
	$\text{W}_{12}\text{O}_{42}^{12-}$ (aq) [10]	$\text{Nb}_2\text{O}_5 \cdot n\text{H}_2\text{O}$ (aq) [13]
aqueous solution	962, 945, 906, —, 615, 560, 366, 310, 225	880, 630, 280
monolayer on Al_2O_3 (ambient conditions)	975, —, 860, 807, 715, 550, 330, 273, 235	890, 650, 230

veals that essentially the same metal oxide species are present in both systems [9–13]. The Raman bands of the hydrated surface species may be slightly shifted from the corresponding aqueous compounds because of minor distortions in the thin aqueous film. Some weak bands may not be detectable because of the background signal from the oxide support. The similar metal oxide species present for the ambient supported metal oxide catalysts and the aqueous solutions suggests that the hydrated surface metal oxide species are not anchored to the oxide support under ambient conditions, but are suspended in the thin aqueous layer.

The specific molecular structures of the hydrated surface metal oxide species are related to the pH of the thin aqueous layer as in conventional aqueous solutions [9–14]. The pH of this aqueous thin film is determined by the net pH at which the surface possesses zero surface charge (the point of zero charge, pzc) which is determined by the specific oxide substrate and the surface coverage of the specific surface metal oxide species. The molecular structures of the hydrated surface metal oxide species can be predicted from their corresponding aqueous phase diagrams [14] and the pH of the aqueous thin film, since the metal oxide species are in thermodynamic equilibrium with the aqueous solution [9–13]. The net pH at the pzc model of the hydrated surface metal oxide species has been confirmed by other molecular spectroscopic characterization studies: solid state ^{51}V NMR [15,16], X-ray absorption near edge spectroscopy (XANES) [17,18] and UV-visible diffuse reflectance spectroscopy (DRS) [19].

The net pH at the pzc model of the hydrated surface metal oxide species also suggests that the preparation method or specific phase of the oxide support (e.g., TiO_2 (anatase) or TiO_2 (rutile)) should not influence the molecular structure of the hydrated surface metal oxide species since it is in thermodynamic equilibrium at the pH of the thin aqueous layer. This statement applies to supported metal oxide systems where the oxide support is preformed, compara-

ble surface coverages are examined, and the catalysts have only received a modest calcination treatment (400–500°C). The mild calcination temperature assures that the surface metal oxide species are fully oxidized and dispersed, and that the formation of solid solutions or compounds are avoided. The influence of preparation method (aqueous impregnation with ammonium heptamolybdate and molybdenum oxalate, equilibrium adsorption, nonaqueous impregnation with Mo-allyl precursors, grafting with MoCl_5 and electrochemical reduction to Mo^{+3}) upon the Raman spectra of hydrated surface molybdenum oxide species on alumina and silica have been extensively investigated and the hydrated surface molybdenum oxide species were found to be independent of the specific preparation method [12,18,20,21]. The major hydrated surface molybdenum oxide species present at high coverages on alumina and silica were $\text{Mo}_8\text{O}_{26}^{4-}$ ($\text{Mo}=\text{O}$ Raman band at 958–960 cm^{-1}) and $\text{Mo}_7\text{O}_{24}^{6-}$ ($\text{Mo}=\text{O}$ Raman band at 946–951 cm^{-1}), respectively. Similar conclusions were reached for titania supported molybdenum oxide and vanadium oxide catalysts when different preparations methods (equilibrium adsorption, grafting, aqueous solutions of ammonium heptamolybdate and molybdenum oxalate, and thermal spreading of crystalline MoO_3 or V_2O_5 powders) were employed [22]. The major hydrated surface molybdenum oxide and vanadium oxide species on titania at high coverages were $\text{Mo}_8\text{O}_{26}^{4-}$ ($\text{Mo}=\text{O}$ Raman band at 960–963 cm^{-1}) and $\text{V}_{10}\text{O}_{28}^{6-}$ ($\text{V}=\text{O}$ Raman band at 989–993 cm^{-1}), respectively. The influence of the specific phase or modification of the oxide support was also investigated for the titania supported vanadia and molybdena catalysts and was not found to influence the nature of the surface vanadia and molybdena species [12,23]. Thus, changing the preparation method or the specific modification of the oxide support does not influence the molecular structure of the hydrated surface metal oxide species since the net pH at pzc is not significantly altered.

Table 2

Raman and IR bands (in cm^{-1}) for dehydrated surface metal oxide species on Al_2O_3 [5]

	10% $\text{MoO}_3/\text{Al}_2\text{O}_3$	5% $\text{WO}_3/\text{Al}_2\text{O}_3$	5% $\text{V}_2\text{O}_5/\text{Al}_2\text{O}_3$
Raman	1000	1010	1025
IR (primary $M=O$ vibration)	1000	1010	1026
IR (first $M=O$ overtone)	1992	2009	2042

3.2. Dehydrated conditions

The hydrated surface metal oxide species present under ambient conditions are only stable in aqueous environments and decompose when the sample is dehydrated [24]. The decomposition is also driven by the reaction of the surface metal oxide species with the surface hydroxyls of the oxide supports (see discussion below). The surface metal oxide species under dehydrated and hydrated conditions are not related as shown by several spectroscopic comparative studies [15–19,24].

Dehydration shortens the terminal $M=O$ bond and generally shifts this vibration to above 1000 cm^{-1} which makes it detectable in the IR as well as the Raman spectra. The shortening of the $M=O$ bond is due to the absence of hydrogen bonding under dehydrated conditions as well as the restructuring of the surface metal oxide species. The IR and Raman band positions above 1000 cm^{-1} of several dehydrated surface metal oxide species on alumina are presented in Table 2. The Raman and IR band

positions of the terminal $M=O$ bonds are the same for each of these dehydrated surface metal oxide species on alumina. This suggests that only mono-oxo surface species, containing only one terminal $M=O$ bond, are present for the alumina supported molybdenum oxide, tungsten oxide and vanadium oxide systems [4,5]. This conclusion is further confirmed by examining the first $M=O$ overtone region ($1800\text{--}2100\text{ cm}^{-1}$ region) in the IR which reveals only one vibrational band (see Table 2). A di-oxo structure would be expected to give rise to several combination bands. The IR spectra and band positions of many surface metal oxide species on alumina and titania can be found in publications of Busca and co-workers [25] and Lavalley and co-workers [26].

Additional support for the conclusion that surface molybdenum oxide, tungsten oxide and vanadium oxide species possess mono-oxo structures comes from oxygen isotope experiments. This conclusion was confirmed for the $\text{WO}_3/\text{Al}_2\text{O}_3$ [27], $\text{V}_2\text{O}_5/\text{TiO}_2$ [28] and $\text{MoO}_3/\text{SiO}_2$ [29] systems. The oxygen isotope experiments demonstrated that only two vibrations were present for these supported metal oxide catalyst systems. This is consistent with mono-oxo structures ($M=^{16}\text{O}$ and $M=^{18}\text{O}$) since di-oxo surface species would be expected to yield three vibrations ($^{16}\text{O}=M=^{16}\text{O}$, $^{18}\text{O}=M=^{18}\text{O}$ and $^{18}\text{O}=M=^{16}\text{O}$). Unfortunately, such informative oxygen isotope experiments are very rare and essentially have not been performed for other supported metal oxide catalyst systems.

Table 3

Raman band (in cm^{-1}) for dehydrated surface metal oxide species on Al_2O_3 [24]

Catalyst	$\nu(M=O)$	$\nu(M-O-M)$ or $\nu(-O-M-O)$	$\delta(M-O)$	$\delta(M-O-M)$
1.3% $\text{Re}_2\text{O}_7/\text{Al}_2\text{O}_3$	1004, 890	–	332	–
9% $\text{CrO}_3/\text{Al}_2\text{O}_3$	1005	880, 770, 600	400	300
10% $\text{MoO}_3/\text{Al}_2\text{O}_3$	1000	870, 580	360	210
15% $\text{WO}_3/\text{Al}_2\text{O}_3$	1010	880, 590	300	215
15% $\text{V}_2\text{O}_5/\text{Al}_2\text{O}_3$	1023, 925	770, 620, 560	340	250
12% $\text{Nb}_2\text{O}_5/\text{Al}_2\text{O}_3$	985, 950, 880	640	300	ca. 200

The IR bands of the dehydrated surface metal oxide species on alumina can not be detected below 1000 cm^{-1} because of the IR absorption of the alumina support. However, these bands are readily detectable in the corresponding Raman spectra and reveal many additional bands in this region due to $M\text{--}O\text{--}M$ and $\text{--}O\text{--}M\text{--}O\text{--}$ vibrations (see assignments in Table 3), which are associated with polymerized surface metal oxide species [11,24,30]. The only surface oxide system that does not exhibit vibrations due to polymerized surface metal oxide systems is alumina supported rhenium oxide. The other supported metal oxide systems do show the presence of polymerized surface metal oxide species and their Raman intensities generally increase with coverage. The relative concentrations of the isolated and polymerized surface metal oxide species are not known since their relative Raman cross sections have not been determined.

Neither Raman or IR spectroscopy provide vibrational information about the $M\text{--}O\text{--}$ support bond under dehydrated conditions. The $M\text{--}O\text{--}$ support bond is not Raman active since it is slightly ionic in character and can not be detected with IR since it should occur in the IR absorption region of the oxide supports ($500\text{--}700\text{ cm}^{-1}$). Consequently, in contrast to the hydrated surface metal oxide species which are not anchored to the support and exhibit all the Raman vibrations, the complete coordination of the dehydrated surface metal oxide species can not be determined from Raman or IR spectroscopy.

Information about the coordination of the dehydrated surface metal oxide species has been obtained from complementary spectroscopies: solid state ^{51}V NMR [15,16], XANES [17,18,31–33] and UV–vis DRS [34]. The coordinations of the dehydrated surface metal oxide species on alumina are summarized in Table 4. At low surface coverages, the dehydrated surface metal oxide species generally tend to possess fourfold coordination and be isolated since Raman does not detect strong $M\text{--}O\text{--}M$ or $O\text{--}M\text{--}O$ vibrations. At high surface coverages, the

Table 4

Coordination of dehydrated surface metal oxide species on alumina

Supported metal oxide catalyst	Low coverage	Monolayer coverage	Ref.
$\text{Re}_2\text{O}_7/\text{Al}_2\text{O}_3$	ReO_4	ReO_4	[31]
$\text{CrO}_3/\text{Al}_2\text{O}_3$	CrO_4	CrO_4	[19,34]
$\text{MoO}_3/\text{Al}_2\text{O}_3$	MoO_4	$\text{MoO}_6, \text{MoO}_4$	[18]
$\text{WO}_3/\text{Al}_2\text{O}_3$	WO_4	WO_6, WO_4	[32,34]
$\text{V}_2\text{O}_5/\text{Al}_2\text{O}_3$	VO_4	$\text{VO}_4, \text{VO}_6^a$	[15,34]
$\text{Nb}_2\text{O}_5/\text{Al}_2\text{O}_3$	NbO_4	NbO_6	[33]

^a possible minor species.

coordination of the dehydrated surface metal oxide species depends on the specific metal oxide and strong Raman signals due to polymerized surface species are usually present. The surface rhenium oxide species on alumina are the only surface metal oxide species that do not possess Raman vibrations due to polymerized surface species and remain isolated at all surface coverages. Fourfold coordination is preferred for surface rhenium oxide, chromium oxide and vanadium oxide species; sixfold coordination is preferred for surface tungsten oxide and niobium oxide species; and comparable amounts of fourfold and sixfold molybdenum oxide species appear to be present at monolayer coverages on alumina. In addition to coordination changes with surface coverage, the coordination of the surface metal oxide species may also depend on the specific oxide support [18]. These characterization studies have revealed that the coordination of the surface metal oxide species depends on the specific metal oxide, its surface coverage and the specific oxide support.

The changes in the coordination and extent of polymerization of the dehydrated surface metal oxide species are reflected in slight modifications in the vibrations of the terminal $M\text{=O}$ bonds. These slight shifts can also be caused by a decrease in the bond angle or in the bond strength of the bridging $\text{--}O\text{--}M\text{--}O\text{--}$ groups. The influence of surface coverage on the Raman vibration of the terminal $M\text{=O}$ bond for several dehydrated surface metal oxide species on alu-

Table 5

Terminal $M=O$ band Raman vibrations (in cm^{-1}) of dehydrated surface metal oxide species on Al_2O_3 as a function of coverage [24]

Catalyst	Low coverage	Monolayer coverage
$\text{MoO}_3/\text{Al}_2\text{O}_3$	993	1002
$\text{WO}_3/\text{Al}_2\text{O}_3$	1004	1020
$\text{V}_2\text{O}_5/\text{Al}_2\text{O}_3$	1015	1025
$\text{Nb}_2\text{O}_5/\text{Al}_2\text{O}_3$	980	988

mina are shown in Table 5. There is approximately a $10\text{--}20\text{ cm}^{-1}$ shift to higher wavenumbers as the surface coverage of the surface metal oxide species is increased [24]. Similar vibrational shifts are detected when the specific oxide support is varied and are presented for a series of dehydrated supported vanadium oxide catalysts in Table 6. The vibration of the terminal $M=O$ bond also slightly shifts to lower wavenumbers, usually by about $2\text{--}5\text{ cm}^{-1}$, with increasing temperature due to thermal effects at elevated temperatures (500 C) [22]. These vibrational shifts are due to minor changes in the $M=O$ bond length as discussed below.

There recently have been many Raman/IR spectroscopy papers comparing the positions of the vibrational bands with the corresponding $M\text{--}O$ bond lengths of crystallographically determined metal oxide compounds. These studies have demonstrated that the $M\text{--}O$ bond lengths directly correlate with the Raman/IR band positions associated with the $M\text{--}O$ stretching frequencies: Mo [36,37], V [38], Nb [39], Bi [40], W [41], Ti [42] and P [43]. Such a correlation is

Table 6

Terminal $V=O$ band Raman vibrations (in cm^{-1}) of dehydrated surface vanadium oxide species as a function of coverage and support [35]

Catalyst	Low coverage	Monolayer coverage
Al_2O_3	1015	1026
ZrO_3	1023	1030
TiO_2	1027	1030
Nb_2O_5	1031	1033
SiO_2	1039	— ^a

^a Monolayer coverage not achievable.

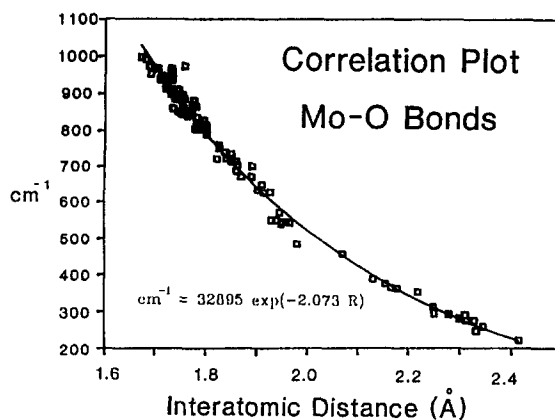


Fig. 3. $\text{Mo}\text{--}O$ bond length vs. Raman stretching frequency relationship.

shown in Fig. 3 for molybdenum oxide reference compounds [36]. It is also possible to determine the relationship between bond order and the $M\text{--}O$ stretching frequency since relationships between the metal–oxygen bond valence and the bond distance have been developed in the literature [44]. The correlation relating the $\text{Mo}\text{--}O$ bond order with the $\text{Mo}\text{--}O$ stretching frequency is presented in Fig. 4. This correlation reveals that $\text{Mo}\text{--}O$ vibrations at approximately 1000 cm^{-1} are associated with terminal $\text{Mo}=\text{O}$ bonds, vibrations at approximately 600 cm^{-1} are associated with single $\text{Mo}\text{--}O$ bonds and vibrations at $100\text{--}300\text{ cm}^{-1}$ are related to partial or long bonds. Such correlations are most accurate at high wavenumber

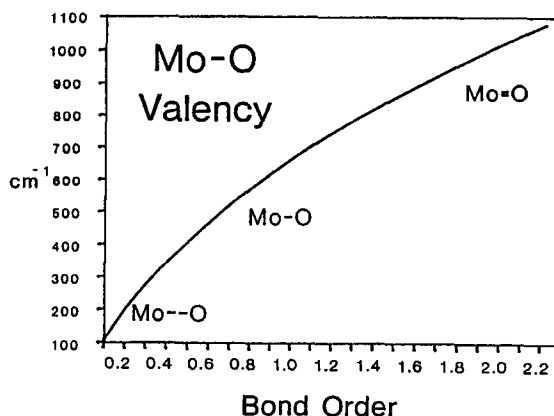


Fig. 4. $\text{Mo}\text{--}O$ bond strength vs. Raman stretching frequency relationship.

regions ($> 800 \text{ cm}^{-1}$) where stretching frequencies are primarily present since at the lower wavenumbers many other vibrational modes are also usually present (see Tables 1 and 2). These correlations reveal that the $10\text{--}20 \text{ cm}^{-1}$ vibrational shifts observed for the terminal $M=O$ bonds of the dehydrated surface metal oxide species, with surface coverage and specific metal oxide support (see Tables 5 and 6), are only due to shortening of the terminal $M=O$ bonds by approximately 0.01 \AA . The several wavenumber shift observed with temperature for the terminal $M=O$ bonds is due to even smaller changes in the bond lengths. The terminal $Mo=O$ bond length was independently determined for the same dehydrated 5.6% MoO_3/SiO_2 sample by Raman and XANES and found to be $1.692 (\pm 0.016) \text{ \AA}$ and $1.690 (\pm 0.02) \text{ \AA}$, respectively [17]. The excellent agreement between these two techniques supports the application of the $M\text{--}O$ stretching frequency correlations for determining the $M\text{--}O$ bond lengths of surface metal oxide species on oxide supports.

The same dehydrated surface metal oxide species were found to be present when various preparation methods were employed to synthesize supported metal oxide catalysts: MoO_3/TiO_2 ($Mo=O$ Raman band at $998\text{--}1001 \text{ cm}^{-1}$) [22], MoO_3/SiO_2 ($Mo=O$ Raman band systematically varied from 975 to 990 cm^{-1} as a function of surface coverage) [45], V_2O_5/TiO_2 ($V=O$ Raman band at $1029\text{--}1032 \text{ cm}^{-1}$) [22] and Nb_2O_5/SiO_2 ($Nb=O$ Raman band at $975\text{--}980 \text{ cm}^{-1}$) [46]. The fact that the same surface metal oxide species can even be formed by thermal treatments of physical mixtures of crystallites of V_2O_5 or MoO_3 with oxide supports such as TiO_2 reveals that these surface metal oxide species spontaneously form or self assemble on oxide supports [1,22]. This suggests that the dehydrated surface metal oxide species possess thermodynamically preferred molecular structures that can not be altered by preparation methods. The specific modification of the titania support (anatase, rutile, brookite and B-phase) was also not found to alter the molecular

structure of the dehydrated surface vanadium oxide species on titania ($V=O$ Raman band varied from $1025\text{--}1031 \text{ cm}^{-1}$ as a function of surface coverage) [23]. Corresponding solid state ^{51}V NMR characterization studies confirmed that the same dehydrated surface vanadium oxide species were present on the different titania support phases [23]. Thus, there is no spectroscopic evidence, as well as catalytic data on well characterized systems [23,45,46], to suggest that the molecular structure of the dehydrated surface metal oxide species is dependent on the specific preparation method.

4. Location of surface metal oxide species

Information about the location of the dehydrated surface metal oxide species on oxide supports can be obtained from in situ IR or Raman spectroscopy investigations that monitor the surface hydroxyl region ($3200\text{--}4000 \text{ cm}^{-1}$). As mentioned above, IR spectroscopy is the preferred vibrational technique for obtaining information about the surface hydroxyl groups. The alumina support contains different surface hydroxyl groups that vibrate between $3400\text{--}3800 \text{ cm}^{-1}$ [6,47]. The IR band at the highest frequency has been assigned to the most basic hydroxyl group and the decrease in frequency of the surface hydroxyls has been associated with increasing acidity [6]. Deposition of metal oxides on alumina reveals that the alumina surface hydroxyls are being consumed and that the consumption of surface hydroxyls proceeds in a sequential fashion: the bands due to the most basic hydroxyls, located at the higher frequencies, disappear first with bands due to neutral and more acidic ones disappearing at higher loadings [47]. For example, see Fig. 5 for the IR spectra of the hydroxyl region for the Re_2O_7/Al_2O_3 system. The broad band centered at about 3590 cm^{-1} is characteristic of residual chemisorbed water due to the mild pretreatment at 300°C . The presence of the adsorbed mois-

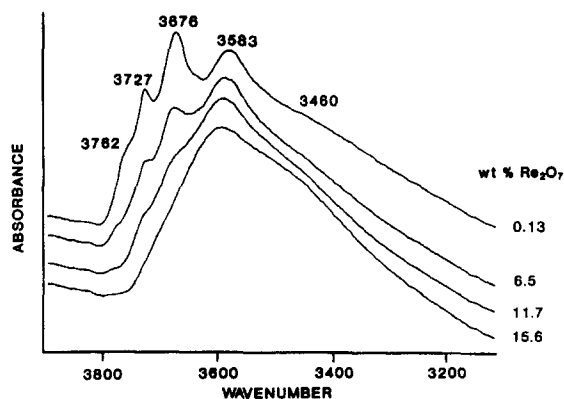


Fig. 5. Infrared hydroxyl region of $\text{Re}_2\text{O}_7/\text{Al}_2\text{O}_3$ as function of rhenium oxide loading (dehydrated at 300°C).

ture also causes the vibrations of OH groups to shift to lower frequency due to hydrogen bonding [6]. Comparison of the quantity of hydroxyls consumed per surface metal oxide species suggests that titration of the supports' reactive hydroxyls is the primary anchoring mechanism of surface metal oxide species [48]. To a lesser extent, however, surface metal oxide species may also become anchored on oxide supports by interacting with exposed Lewis cation sites [49] or by breaking $M\text{--O--}M$ bonds of the oxide support [16]. Thus, IR and Raman studies directly demonstrate that the dehydrated surface metal oxide species primarily anchor to the oxide supports by titrating the surface hydroxyl sites and, consequently, the surface metal oxide species are located on the surface of the oxide supports.

5. Surface coverage of surface metal oxide species

In principle, it should be possible to determine monolayer surface coverage of the surface metal oxide species from IR experiments since complete consumption of surface hydroxyls of the oxide support should correspond to monolayer coverage. However, the IR signal of the surface hydroxyls decreases somewhat more

rapidly than the increasing surface metal oxide coverages [47]. For example, the IR spectra of the alumina supported rhenium oxide catalyst in Fig. 5 exhibits very few surface hydroxyls at 11.7% Re_2O_7 and this loading corresponds to only about a third of a monolayer. This trend may be due to broadening of the surface hydroxyl IR signals at high surface metal oxide coverages, which makes it more difficult to detect their IR signals. CO_2 chemisorption on oxide supports, monitored by IR spectroscopy, also generally provides qualitative information about the surface metal oxide coverage on oxide supports because of its preferential chemisorption on the more basic hydroxyls that are usually titrated at low surface coverages [47,50]. Thus, only qualitative information about the surface coverage of surface metal oxide species on oxide supports can generally be obtained with IR spectroscopy.

Quantitative determination of the surface coverage of the surface metal oxide species on oxide supports can usually be obtained from Raman spectroscopy measurements because of its ability to discriminate between surface metal oxide species and microcrystalline metal oxides. For many supported metal oxide systems (e.g., metal oxides deposited on alumina, titania, zirconia and niobia), the surface metal oxide species is preferentially formed up to monolayer coverage. At monolayer coverage, all the reactive surface hydroxyls of the support have been titrated and deposition of additional metal oxide results in the formation of microcrystalline metal oxide particles. Thus, the appearance of microcrystalline metal oxide particles reflects the titration point of the surface hydroxyls of the oxide support and achievement of monolayer coverage. Raman is very sensitive to the appearance of the microcrystalline metal oxide particles since their Raman cross sections are usually orders of magnitude greater than that of the surface metal oxide species [51] and the major vibrations of the microcrystals (e.g., MoO_3 (815 cm^{-1}), WO_3 (808 cm^{-1}), V_2O_5 (994 cm^{-1}) and Nb_2O_5 (680 cm^{-1})) usually occur at differ-

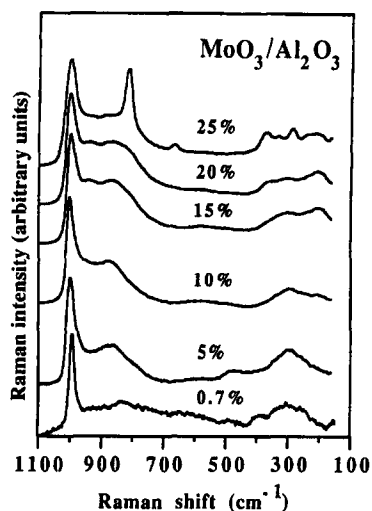


Fig. 6. Raman spectra of supported $\text{MoO}_3/\text{Al}_2\text{O}_3$ as a function of molybdenum oxide loading (dehydrated at 500°C).

ent frequencies than the strongest vibrations of the surface metal oxide species (typically above 1000 cm^{-1} , see Table 2, Table 3, Tables 5 and 6). For example, the Raman spectra of a series of dehydrated $\text{MoO}_3/\text{Al}_2\text{O}_3$ catalysts are shown as a function of surface coverage in Fig. 6: only the Raman bands due to the surface metal oxide species are present from 0.7%–20% MoO_3 (1002 , 940 , 870 , 360 , 300 and 210 cm^{-1}) and the presence of crystalline MoO_3 above monolayer coverage is readily detected by the additional Raman bands at 815 , 665 and 280 cm^{-1} .

Monolayer coverages of several surface metal oxides on different oxide supports were determined by Raman spectroscopy and are pre-

sented in Table 7. For many of the alumina supported metal oxide systems, monolayer coverage corresponds to approximately $4\text{--}5\text{ atoms/nm}^2$. However, the surface coverage for the alumina supported rhenium oxide system is approximately half of this value and the surface coverage of the alumina supported vanadium oxide system is about double this value. The low surface density of the surface rhenium oxide species on alumina is a consequence of the volatility of the surface rhenium oxide species when Re_2O_7 dimers are formed [30]. The high surface density of the surface vanadium oxide species on alumina reflects the ability of this oxide to pack more densely on the surface. Comparison of monolayer coverages on alumina with other oxide supports such as titania, zirconia and niobia reveals that comparable surface densities are achieved on all these oxide supports and is not unique to any specific support. The slightly higher values for monolayer coverages of surface chromia and niobia on the titania and zirconia supports is related to the difficulty in detecting the corresponding crystallites because of overlap with the oxide support Raman bands. Note that monolayer coverages of these surface metal oxide overlayers on alumina, titania, zirconia and niobia are somewhat lower than monolayer coverages for metal catalysts, typically taken as approximately $11\text{--}12\text{ atoms/nm}^2$ [52], because of the relatively large size of these metal–oxo complexes that possess several $M\text{--O}$ support bonds.

The maximum surface coverages of the surface metal oxides on silica are significantly less than that observed on the other oxide supports and are usually about an order of magnitude lower (see Table 7). The low surface coverages on silica are due to the somewhat lower density and reactivity of the silica surface hydroxyls relative to the other oxide supports. Furthermore, silica does not even appear to hold on to these surface metal oxide species very strongly since physical mixtures of silica supported surface metal oxide species with other oxide supports (alumina, titania, etc.) results in complete

Table 7
Monolayer surface coverages of supported metal oxide catalysts (atoms/nm^2)

	Al_2O_3	TiO_2	ZrO_2	Nb_2O_5	SiO_2	Ref.
Re	2.3	2.4	3.3	—	0.54	[30]
Cr	4.0	6.6	9.3	—	0.6	[5]
Mo	4.6	4.6	4.3	4.6	0.3	[18]
W	4.0	4.2	4.0	3.0	0.1	—
V	7.3	7.9	6.8	8.4	0.7	[35]
Nb	4.8	5.8	5.8	—	0.3	[13]

migration of the surface metal oxide species from silica to the other oxide support during thermal treatments [34,53]. Certain preparation methods, however, can enhance the surface coverages of the surface metal oxide species on silica [16,17,34,45,46,54,55]. These preparation methods involve the use of silica supports that possess a high surface concentration of hydroxyls [16,34,45], nonaqueous preparations involving organometallic precursors [46,54,55] and electrochemical deposition of oxides in reduced oxidation states [17]. These preparation methods, however, only increase the surface coverages to approximately a quarter of a monolayer and do not change the molecular structures of the surface metal oxide species. Thus, the somewhat lower surface reactivity of the silica support relative to other oxide supports (alumina, titania, zirconia and niobia) prevents the formation of a complete monolayer of surface metal oxide species on silica.

6. Surface Brønsted and Lewis acid sites

Chemisorption of basic probe molecules followed by IR or Raman is usually an informative approach to determine the nature of surface Lewis and Brønsted acid sites present on oxide surfaces [6,7,56,57]. IR spectroscopy is usually the preferred measurement method in such investigations because of potential fluorescence problems with such Raman spectroscopy measurements. Pyridine is a typical probe molecule in such IR studies since its ring-stretching vibrational modes (originally at 1439 and 1583 cm^{-1}) are affected by becoming coordinately bonded to surface Lewis acid sites (PyL: observed at 1440–1460 and 1600–1635 cm^{-1}) or forming a pyridinium ion at surface Brønsted acid sites (PyH⁺: observed at 1535–1550 and about 1640 cm^{-1}). The concentration of surface Lewis and Brønsted acid sites can also be determined from the intensities of the PyL and PyH⁺ IR bands and their extinction coefficients after saturation of all the surface sites [49].

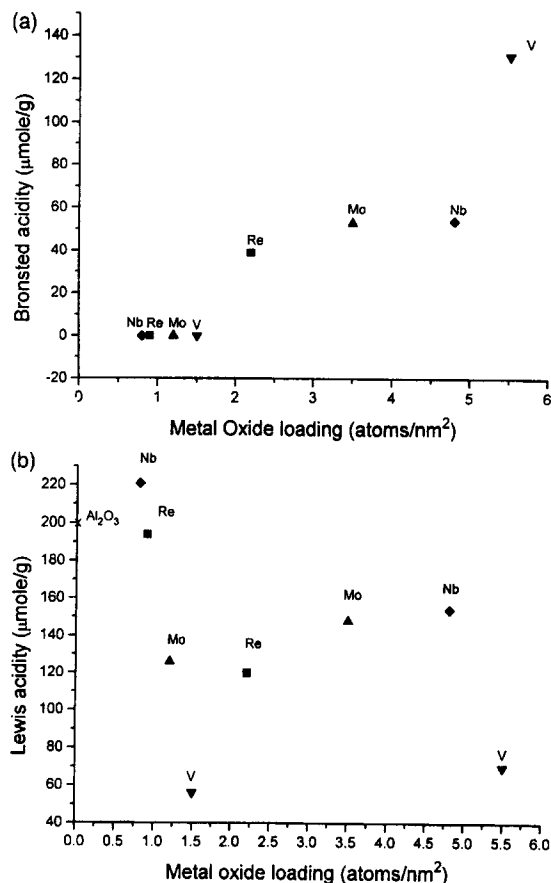


Fig. 7. (a) Brønsted acidity of supported metal oxide species on Al₂O₃ (dehydrated at 425°C). (b) Lewis acidity of supported metal oxide species on Al₂O₃ (dehydrated at 425°C).

The distribution of surface Lewis and Brønsted acid sites for alumina supported metal oxide catalysts have been extensively investigated [47,49,58]. The alumina support only possesses Lewis acid sites and low concentrations of surface metal oxide species do not significantly affect the number of such sites. At high loadings of surface metal oxides on alumina, however, the number of surface Lewis acid sites can appreciably decrease and surface Brønsted acid sites are also present. The number of surface Lewis and Brønsted acid sites for the alumina supported metal oxide catalysts are shown in Fig. 7a and Fig. 7b as a function of surface coverage [47]. It appears that there is a universal curve for the number of surface Brønsted acid sites since it is only dependent on the surface

density of the surface metal oxide species. Note that the high surface densities achieved by the alumina supported vanadium oxide species (see Table 7) results in the highest number of surface Brønsted acid sites. This acidity pattern does not appear to be related to changes in the coordination of the surface metal oxide species since rhenium oxide possesses four-fold coordination at all coverages and both four-fold and six-fold coordinated species are present at high surface coverages (see Table 4). At monolayer coverages, the fraction of surface metal oxide species possessing Brønsted acidity only corresponds to about 5–10% of the sites. It has been proposed that the surface Brønsted acid site is located at the bridging $M-O$ -support bond [47], but direct spectroscopic evidence for the location of the Brønsted acid sites in supported metal oxide catalysts is currently not available. The Lewis acidity of the alumina supported metal oxide species decreases from the value of the pure alumina support (Fig. 7b). The decrease in the Lewis acidity appears to follow the trend of the supported metal oxide loading (atoms/nm²), except for alumina supported vanadium oxide catalysts where a greater than normal reduction in Lewis acidity is observed.

The specific oxide support also affects the surface Brønsted acidity of the surface metal oxide species [49]. For example, supported niobium oxide catalysts only exhibit surface Brønsted acid sites for high coverages on alumina and not for titania, zirconia and silica. Surface Brønsted acid sites do not exist for the silica supported surface metal oxide systems discussed in this paper (Re, Cr, Mo, W, V and Nb). The absence of surface Brønsted acid sites for these silica supported metal oxide systems may be partly related to the low surface densities achievable for the surface metal oxide species on the silica support (see Table 7). Thus, the presence of surface Brønsted acid sites for supported metal oxide catalysts depends on both the specific oxide support ligand and the surface density of the metal oxide overlayer.

7. In situ studies during reactions

Optical spectroscopies such as Raman and IR are ideally suited for investigating the nature of surface metal oxide species as well as adsorbed surface intermediates during catalytic reactions. IR studies of the reactive adsorption of organic molecules on oxides and Raman studies of adsorbed molecules on oxides will be covered in separate papers in this issue of Catalysis Today by Busca and Hendra, respectively. Consequently, the discussion below will primarily be limited to the nature of surface metal oxide species on oxide supports during catalytic reactions. Raman spectroscopy is ideally suited to investigate the behavior of surface metal oxide species during catalytic reactions since there is very little scattering from the gas phase. In the past few years, several in situ Raman spectroscopy investigations during catalytic reactions over supported metal oxide catalysts have been performed [59–66].

Moisture is usually present during many catalytic reactions as a component of the feed or as a product of the reaction (especially oxidation reactions). The above discussions demonstrated that the surface metal oxide species can be present as hydrated structures, under ambient conditions, or dehydrated structures, under in situ conditions where moisture has been desorbed (see Section 3). However, no information is currently available about the influence of moisture at elevated temperatures on the nature of the surface metal oxide species. The influence of flowing a moisture saturated oxygen/helium stream, containing approximately 8% H₂O, over a series of supported vanadium oxide catalysts was investigated over the temperature range 120–500°C [59]. Above 300°C, the surface vanadium oxide species retained their molecular structures and the Raman band of the terminal V=O bonds shifted downward by several cm⁻¹. The slight shift is due to the hydrogen bonding of small amounts of moisture present on the surface at these elevated temperatures. This small shift also indicates that

moisture can compete with the reactants for adsorption on the surface metal oxide species and accounts for the observation that moisture generally inhibits catalytic oxidation reactions over oxide catalysts. At approximately 200°C and below, the surface vanadium oxide species became hydrated and the Raman band of the terminal V=O bonds significantly shifted downward. Thus, at these lower temperatures the surface vanadium oxide species are extensively solvated and would not be expected to be accessible for gas phase catalytic oxidation reactions. An exception to this trend was observed for silica supported vanadium oxide catalysts where the surface vanadium oxide species remained dehydrated over the entire temperature range due to the hydrophobic nature of the silica surface employed.

The oxidation state of surface redox sites such as molybdenum and vanadium oxide catalysts can also be affected during catalytic oxidation reactions and is sensitive to the specific reaction environment. In situ Raman spectroscopy measurements during the selective catalytic reduction of NO by NH₃ over titania supported vanadium oxide catalysts at 400°C revealed that the surface vanadium oxide species remained in a nearly fully oxidized state [60]. However, in situ Raman measurements during methanol oxidation over a series of supported vanadium oxide [61] and molybdenum oxide [62] catalysts showed that a fraction of the surface metal oxide species were reduced under reaction conditions. The influence of the methanol oxidation reaction upon the Raman spectrum of the alumina supported molybdenum oxide catalyst is presented in Fig. 8. Note that during methanol oxidation the Raman intensity of the terminal Mo=O bond, associated with Mo⁶⁺, is diminished and new Raman bands appear at lower wavenumbers (840, 760, 491 and 274 cm⁻¹) which are characteristic of reduced surface molybdenum oxide species. The extent or fraction reduction of the surface molybdenum oxide and vanadium oxide species during methanol oxidation was not a function of

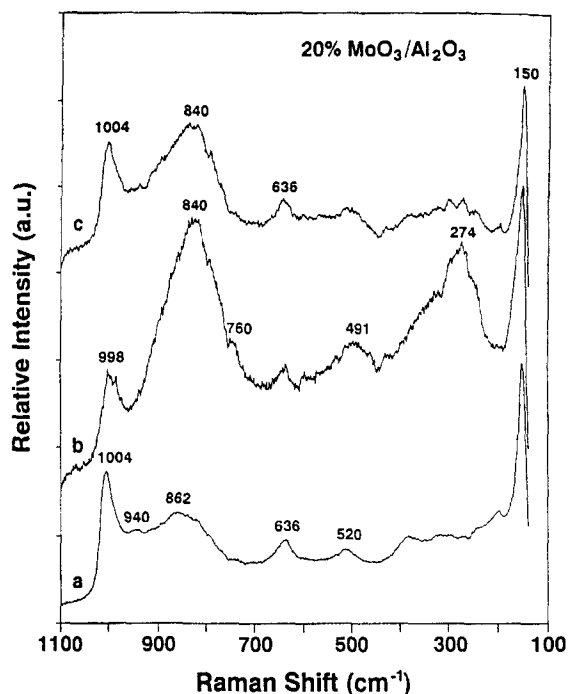


Fig. 8. In situ Raman spectra of MoO₃/Al₂O₃ catalyst during methanol oxidation reaction at 230°C: (a) He/O₂, (b) He/O₂/CH₃OH and (c) He/O₂.

the specific oxide support [61,62]. This suggests that the significant changes in reactivity, several orders of magnitude in the methanol oxidation turnover frequency, as a function of the specific oxide support [61] is primarily due to the reactivity per surface vanadium or molybdenum oxide site rather than the number of sites participating at steady state. Furthermore, it reveals that the oxide support cations behave as important ligands that can influence the reactivity of the surface metal oxide species during redox reactions.

The surface metal oxide species on oxide supports may also structurally transform in certain reactive environments. The surface molybdenum oxide species on silica is not stable during methanol oxidation and transforms to crystalline β -MoO₃ (the low temperature structure of crystalline MoO₃) as shown in Fig. 9 [45]. The 978 cm⁻¹ Raman band due to the dehydrated surface molybdenum oxide species is converted to a series of Raman bands at 894,

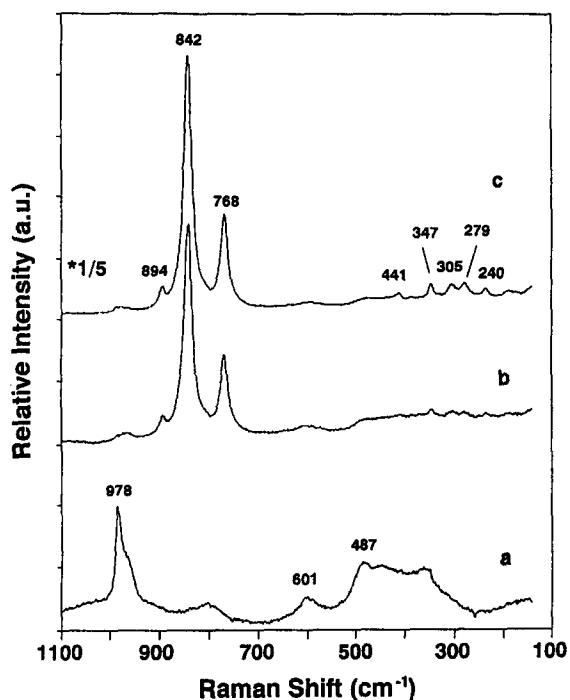


Fig. 9. In situ Raman spectra of $\text{MoO}_3/\text{SiO}_2$ catalyst during methanol oxidation at 230°C : (a) He/O_2 , (b) $\text{He}/\text{O}_2/\text{CH}_3\text{OH}$ and (c) He/O_2 .

842 , 768 and $200\text{--}400\text{ cm}^{-1}$ of crystalline $\beta\text{-MoO}_3$ during methanol oxidation. This structural transformation occurs because of the formation of Mo-methoxy complexes during methanol oxidation over silica supported molybdenum oxide catalysts and is not observed for other supported molybdenum oxide and vanadium oxide catalyst systems. However, the formation of Re-methoxy complexes during methanol oxidation over silica supported rhenium oxide results in the complete volatilization of the surface rhenium oxide species from the silica surface [63]. Surface silicomolybdic acid clusters, $\text{H}_4\text{SiMo}_{12}\text{O}_{40}$, can be formed on silica by exposing silica supported molybdenum oxide catalysts to saturated moisture at room temperature for extended periods of time [64]. The surface silicomolybdic acid clusters form at these conditions via the initial dissolution of the Mo and Si species into the thin aqueous film and the subsequent reaction in the aqueous environment. The surface silicomolybdic acid clusters on silica are stable until approximately

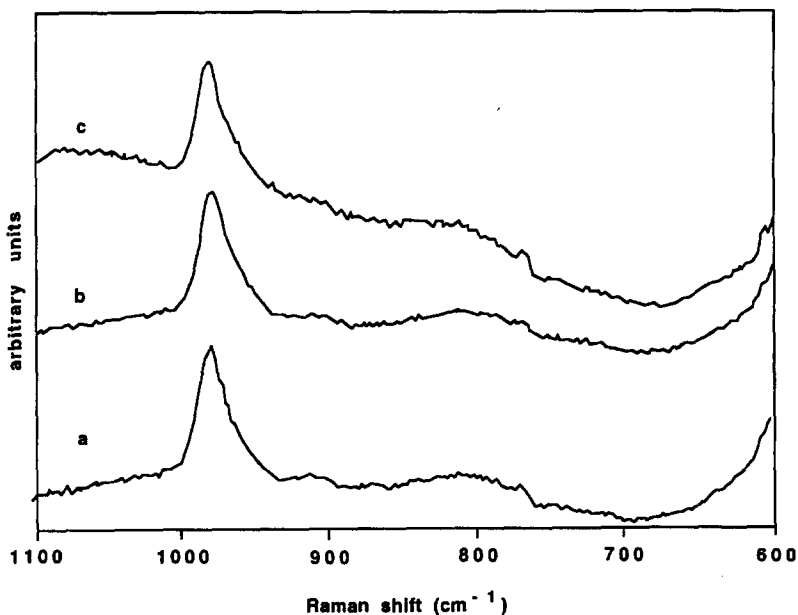


Fig. 10. In situ Raman spectra of $\text{MoO}_3/\text{SiO}_2$ catalyst during methane oxidation (a) $\text{CH}_4/\text{O}_2/\text{He}$ at 550°C , (b) He/O_2 at 550°C and (c) He/O_2 at 25°C .

300°C at which point they decompose to form dehydrated surface molybdenum oxide species. The surface molybdenum oxide species on silica, however, are stable during methane oxidation to formaldehyde at elevated temperatures (see Fig. 10) [65]. This in situ Raman spectrum reveals that the surface molybdenum oxide species on silica is isolated and fully oxidized during methane oxidation. Similar observations have been made for methane oxidation over silica supported vanadium oxide catalysts [66].

In summary, the in situ Raman studies of the surface metal oxide species during reactions reveal that the oxidation states and structures of the surface metal oxide species can be altered by the reaction environment. The changes observed are both a function of the specific supported metal oxide catalyst system and the specific reaction environment. Such fundamental information is critical for the development of structure–reactivity relationships for supported metal oxide catalysts.

8. Historical perspective

The primary objective of this paper is to demonstrate the types of fundamental information that can currently be obtained from Raman/IR characterization of supported metal oxide catalysts and not to be a review of the literature which can be found elsewhere [6,67,68]. However, it is important to acknowledge the contributions of the various research groups in advancing the fundamental understanding of supported metal oxide catalysts through the use of Raman and IR characterization studies.

The first attempt to obtain a Raman spectrum of a supported molybdenum oxide catalyst was reported by Villa et al. in 1974, but a Raman spectrum could not be obtained [69]. Fortunately, several successful studies of Raman spectra of supported molybdenum oxide and tungsten oxide catalysts appeared in 1977 by Brown et al. [70–72], Thomas et al. [73] and de

Vries et al. [74]. The first Raman spectra of supported vanadium oxide and rhenium oxide catalysts were reported in the following years by Roozeboom et al. [75] and Kerkhof et al. [76], respectively. Iannibello et al. [77] reported the initial Raman spectra of supported chromium oxide catalysts and Jehng et al. [78] reported the first Raman spectra of supported niobium oxide catalysts. Other research groups that made significant contributions during this period were Knozinger and Jeziorowski [79,80], Bonelle and co-workers [81], Cheng and Schrader [82] and Wang and Hall [83]. This early stage of Raman spectroscopy of supported metal oxide catalysts is extensively reviewed in recent publications [67,68]. The above studies, however, were all performed under ambient conditions where the surfaces were hydrated. Subsequent Raman studies by Deo and Wachs [9] demonstrated that the molecular structures of the hydrated surface metal oxide species under ambient conditions are directly related to the net surface pH at pzc of the thin aqueous layer.

The realization that the molecular structures of the surface metal oxide species are hydrated under ambient conditions lead to in situ Raman studies that attempted to determine the structures of the dehydrated surface metal oxide species. The first in situ Raman studies appeared in 1983 and were performed by Wang and Hall on supported rhenium oxide catalysts [84] and by Schrader and Cheng who reported on the sulfidation of alumina supported molybdenum oxide catalysts [85]. In the subsequent year, several more in situ Raman studies appeared in the literature: Chan et al. reported the dehydrated spectra of supported vanadium oxide, tungsten oxide and molybdenum oxide catalysts [86] and Stencel et al. reported the dehydrated spectra of supported molybdenum oxide [87] and tungsten oxide catalysts [27]. The first dehydrated Raman spectra of supported chromium oxide catalysts were first reported by Hardcastle and Wachs in 1988 [88] and that of supported niobium oxide catalysts by Jehng and Wachs in 1991 [89]. These in situ Raman stud-

ies clearly showed that different surface metal oxide species were present under ambient and dehydrated conditions. In order to obtain additional molecular structural information about the dehydrated surface metal oxide species subsequent studies coupled the Raman characterization studies with other molecular spectroscopies (e.g., IR [5,28,30], EXAFS/XANES [17,18,31,32], UV-Vis DRS [34,53], and solid state NMR [16,23]). Recently, the European catalysis community collaborated to characterize V_2O_5/TiO_2 catalysts with numerous spectroscopies and this project represents the most extensive characterization of supported metal oxide catalysts [90].

The corresponding IR characterization studies of the $M=O$ vibrations of supported metal oxide catalysts also appeared in the literature during the same time period. Many of the initial IR studies usually presented dehydrated spectra because of the commercial availability of in situ IR cells. The first successful IR investigation of supported metal oxide catalysts was reported in 1974 by Mitchell and Trifiro for hydrated supported molybdenum oxide catalysts [91]. The dehydrated IR spectra of supported chromium oxide catalysts was reported by Zecchina et al. in the following year [92]. Nakamura et al. reported the first in situ IR study of supported rhenia catalysts in 1981 [93]. The first IR spectra of hydrated supported vanadium oxide catalysts were published by Nakagawa et al. in 1983 [94]. The following year, Lavalley and co-workers reported the in situ IR spectra of supported molybdenum oxide and tungsten oxide catalysts [26]. The first dehydrated Raman spectra of supported vanadium oxide catalysts were reported by Lavalley and co-workers in 1986 [26]. Lavalley and co-workers also demonstrated that fundamental information about the $M=O$ vibrations can also be obtained in the first overtone region of the IR spectrum [26]. IR spectra of hydrated or dehydrated supported niobia catalysts have not been reported in the literature to date, but their vibrations can be

predicted from the corresponding Raman bands presented in Table 1, Table 3 and Table 5.

Additional information about the surface chemistry of supported metal oxide catalysts was also obtained from in situ IR studies. Information about the interaction of the surface metal oxide species with the surface hydroxyls of the oxide support was initially demonstrated by Sonnemans and Mars in 1973 [95]. It was subsequently quantified that 1–2 surface hydroxyls are consumed by one surface molybdenum oxide species [48]. The first application of pyridine adsorption to measure the distribution of surface Lewis and Brønsted acid sites of supported molybdenum oxide catalysts was reported by Kiviat and Petrakis [96] and extensively applied by Segawa and Hall to many different supported metal oxide catalysts [58]. Chemisorption of CO_2 on the exposed portion of the oxide support to estimate the surface coverage of surface metal oxide species was developed by Segawa and Hall [97].

In situ IR studies during reactions have received much attention in the literature (see paper by Busca and Hendra in this issue of Catalysis Today). However, only a handful of in situ Raman studies of supported metal oxide catalysts during reactions have appeared to date and are discussed above. In the next few years, the focus of many in situ studies will be to characterize the surface metal oxide species and adsorbed intermediates during catalytic reactions.

9. Conclusions

The complementary nature of Raman and IR spectroscopy is reflected in the above review of the characterization of supported metal oxide catalysts. The molecular structures of the surface metal oxide species under ambient conditions, where the surface is hydrated with a thin aqueous layer, are determined by the net pH at the pzc of the supported metal oxide system. The molecular structures under dehydrated con-

ditions are spontaneously formed by self assembly and can not be influenced by preparation methods. The dehydrated molecular structures are both a function of surface coverage and the specific oxide support. The surface metal oxide species primarily coordinate to the oxide supports by titrating the surface hydroxyls of the supports. Monolayer coverage of the surface metal oxide species generally corresponds to approximately 4–5 atoms/nm² for alumina, titania, zirconia and niobia supports. The surface density of surface rhenium oxide species is usually less due to volatilization and the surface density of surface vanadium oxide species is usually higher because of its ability to pack more densely. Monolayer coverage of surface metal oxide species on silica can not be achieved and surface densities of 0.1–1 atoms/nm² are typically obtained. For silica supported metal oxide catalysts, the surface density is influenced by the preparation method but not the molecular structures. The number of surface Brønsted acid sites is determined by the specific oxide support and the surface coverage of the surface metal oxide species. Under reaction conditions, the surface metal oxide species can be unchanged, hydrated, reduced to a lower oxidation state or transformed to a crystalline phase. These changes depend on the specific supported metal oxide system and the specific reaction environment. Such fundamental information is critical for the development of molecular–structure reactivity relationships for supported metal oxide catalysts.

Acknowledgements

This paper is dedicated to my former and current students at Lehigh University who have contributed to advancing the catalysis science of surface metal oxides on oxide supports (F.D. Hardcastle, J.-M. Jehng, G. Deo, M.A. Vuurman, D.S. Kim, A.M. Turek, H. Hu, M.A. Banares, M. Ostromecki, N. Arora and M. Kellner).

References

- [1] Y.-C. Xie and Y.-Q. Tang, *Adv. Catal.*, 37 (1990) 1.
- [2] C.L. Thomas, *Catalytic Processes and Proven Catalysts*, Academic Press, New York, 1970.
- [3] I.E. Wachs and K. Segawa, in I.E. Wachs (Editor), *Characterization of Catalytic Materials*, Butterworth-Heinemann, Boston, 1992, Chapter 4.
- [4] K. Nakamoto, *Infrared and Raman Spectra of Inorganic and Coordination Compounds*, 4th edition, Wiley, New York, 1977.
- [5] M.A. Vuurman, Ph. D. Dissertation, University of Amsterdam, The Netherlands, 1992.
- [6] H.-P. Boehm and H. Knozinger in J.R. Anderson and M. Boudart (Editors), *Catalysis*, Vol. 4, Springer, Berlin, 1983, Chapter 2.
- [7] R.M. Pittman and A.T. Bell, *Catal. Lett.*, 24 (1993) 1.
- [8] P.F. McMillan and R.L. Remmele, *Am. Miner.*, 71 (1986) 772.
- [9] G. Deo and I.E. Wachs, *J. Phys. Chem.*, 95 (1991) 5889.
- [10] S.D. Kohler, J.G. Ekerdt, D.S. Kim and I.E. Wachs, *Catal. Lett.*, 16 (1992) 231.
- [11] M.A. Vuurman, F.D. Hardcastle and I.E. Wachs, *J. Mol. Catal.* 84 (1993) 193.
- [12] D.S. Kim, K. Segawa, T. Soeya and I.E. Wachs, *J. Catal.*, 136 (1992) 539.
- [13] J.-M. Jehng and I.E. Wachs, *J. Mol. Catal.*, 67 (1991) 369.
- [14] C.F. Baes, Jr. and R.E. Mesmer, *The Hydrolysis of Cations*, Wiley, New York, 1970.
- [15] H. Eckert and I.E. Wachs, *J. Phys. Chem.*, 93 (1989) 6796.
- [16] N. Das, H. Eckert, H. Hu, I.E. Wachs, J. Walzer and F. Feher, *J. Phys. Chem.*, 97 (1993) 8240.
- [17] M. de Boer, A.J. van Dillen, D.C. Koningsberger, J.W. Geus, M.A. Vuurman and I.E. Wachs, *Catal. Lett.*, 11 (1991) 227.
- [18] H. Hu, I.E. Wachs and S.R. Bare, *J. Phys. Chem.*, in press.
- [19] B.M. Weckhuysen, L.M. De Ridder and R.A. Schoonheydt, *J. Phys. Chem.*, 97 (1993) 4756.
- [20] C.C. Williams, J.G. Ekerdt, J.-M. Jehng, F.D. Hardcastle, A.M. Turek and I.E. Wachs, *J. Phys. Chem.*, 95 (1991) 8781.
- [21] C.C. Williams, J.G. Ekerdt, J.-M. Jehng and I.E. Wachs, *J. Phys. Chem.*, 95 (1991) 8791.
- [22] T. Machej, J. Haber, A.M. Turek and I.E. Wachs, *Appl. Catal.*, 70 (1991) 115.
- [23] G. Deo, A.M. Turek, I.E. Wachs, T. Machej, J. Haber, N. Das, H. Eckert and A.M. Hirt, *Appl. Catal. A: General*, 91 (1992) 27.
- [24] M.A. Vuurman and I.E. Wachs, *J. Phys. Chem.*, 96 (1992) 5008.
- [25] G. Busca, *Mat. Chem. Phys.*, 19 (1988) 157; F. Mange, J.-P. Gallas, J.C. Lavalley, G. Busca, G. Ramis and V. Lorenzelli, *Mikrochim. Acta II*, (1988) 57; C. Cristiani, P. Forzatti and G. Busca, *J. Catal.*, 116 (1989) 588; G. Ramis, G. Busca and F. Bregani, *Catal. Lett.*, 18 (1993) 299.
- [26] M. Cornac, A. Janin and J.C. Lavalley, *Infrared Phys.*, 24 (1984) 143; D. Quafi, A. Janin and J.C. Lavalley, *Proc. 10th Int. Symp. React. Solids*, Elsevier, Dijon, 1984, p. 1015; G. Busca and J.C. Lavalley, *Spectrochim. Acta*, 42A (1986) 443.

- [27] J.M. Stencel, L.E. Makovsky, J.R. Diehl and A.T. Sarkus, *J. Raman Spectrosc.*, 15 (1984) 282.
- [28] G. Ramis, C. Cristiani, P. Forzatti and G. Busca, *J. Catal.*, 124 (1990) 574.
- [29] M. Cornac, A. Janin and J.C. Lavalley, *Polyhedron*, 5 (1986) 183.
- [30] M.A. Vuurman, D.J. Stufkens, A. Oskam and I.E. Wachs, *J. Mol. Catal.*, 76 (1992) 263.
- [31] F.D. Hardcastle, I.E. Wachs, J.A. Horsley and G.H. Via, *J. Mol. Catal.*, 46 (1988) 15.
- [32] J.A. Horsley, I.E. Wachs, J.M. Brown, G.H. Via and F.D. Hardcastle, *J. Phys. Chem.*, 91 (1987) 4014.
- [33] S. Yoshida and I.E. Wachs, to be submitted to *Catal. Today*.
- [34] B.M. Weckhuysen, G. Deo and I.E. Wachs, to be published.
- [35] G. Deo and I.E. Wachs, *J. Catal.*, 146 (1994) 323.
- [36] F.D. Hardcastle and I.E. Wachs, *J. Raman Spectrosc.*, 21 (1990) 683.
- [37] F.A. Cotton and R.M. Wing, *Inorg. Chem.*, 4 (1965) 867.
- [38] F.D. Hardcastle and I.E. Wachs, *J. Phys. Chem.*, 95 (1991) 5031.
- [39] F.D. Hardcastle and I.E. Wachs, *Solid State Ionics*, 45 (1991) 201.
- [40] F.D. Hardcastle and I.E. Wachs, *J. Solid State Chem.*, 97 (1992) 319.
- [41] F.D. Hardcastle and I.E. Wachs, *J. Raman Spectrosc.*, in press.
- [42] F.D. Hardcastle and I.E. Wachs, submitted to *J. Phys. Chem.*
- [43] A. Rulmont, R. Cahay, M. Liegeois-Duyckaerts and P. Tarte, *Eur. J. Solid State Inorg. Chem.*, 28 (1991) 207.
- [44] I.D. Brown and K.K. Wu, *Acta Cryst.*, B32 (1976) 1957.
- [45] M.A. Banares, H. Hu and I.E. Wachs, *J. Catal.*, 150 (1994) 407.
- [46] J.-M. Jehng and I.E. Wachs, *Catal. Today*, 16 (1993) 417.
- [47] A.M. Turek, I.E. Wachs and E. DeCanio, *J. Phys. Chem.*, 96 (1992) 5000.
- [48] W.S. Millman, M. Crespin, A.C. Cirillo, S. Abdo and W.K. Hall, *J. Catal.*, 60 (1979) 404; V.M. Mastikhin, A. Nosov, V.V. Terskikh, K.I. Zamaraev and I.E. Wachs, *J. Phys. Chem.*, 98 (1994) 13621.
- [49] J. Datka, A.M. Turek, J.-M. Jehng and I.E. Wachs, *J. Catal.*, 135 (1992) 186.
- [50] F.M. Mulcahy, K.D. Kozminski, J.M. Slike, F. Ciccone, S. J. Scierka, M.A. Eberhardt, M. Houlla and D.M. Hercules, *J. Catal.*, 139 (1993) 688.
- [51] S.S. Chan, I.E. Wachs and L.L. Murrell, *J. Catal.*, 90 (1984) 150.
- [52] M. Boudart and G. Djéga-Mariadassou, in *Kinetics of Heterogeneous Catalytic Reactions*, Princeton University Press, Princeton, 1984.
- [53] J.-M. Jehng, I.E. Wachs, B.M. Weckhuysen and R.A. Schoonheydt, *J. Chem. Soc., Faraday Trans.*, 91 (1994) 953.
- [54] R.D. Roark, S.D. Kohler, J.G. Ekerdt, D.S. Kim and I.E. Wachs, *Catal. Lett.*, 16 (1992) 77.
- [55] D.S. Kim, M. Ostromecki, I.E. Wachs, S.D. Kohler and J.G. Ekerdt, *Catal. Lett.*, 33 (1995) 209.
- [56] R. Ferwerda, J.H. van der Maas and P.J. Hendra, *J. Phys. Chem.*, 97 (1993) 7331.
- [57] R. Ferwerda, J.H. van der Maas and P.J. Hendra, *Vib. Spectrosc.*, 7 (1994) 37.
- [58] K. Segawa and W.K. Hall, *J. Catal.*, 76 (1982) 133.
- [59] J.-M. Jehng, G. Deo and I.E. Wachs, submitted to *J. Mol. Catal.*
- [60] G.T. Went, L.-J. Leu, R.R. Rosin and A.T. Bell, *J. Catal.*, 134 (1992) 492.
- [61] G. Deo and I.E. Wachs, to be published
- [62] H. Hu and I.E. Wachs, *J. Phys. Chem.*, 99 (1995) 10911.
- [63] J.-M. Jehng and I.E. Wachs, to be published.
- [64] M.A. Banares, H. Hu and I.E. Wachs, *J. Catal.*, 155 (1995) 249.
- [65] M.A. Banares, M.D. Jones, N.D. Spencer and I.E. Wachs, *J. Catal.*, 146 (1994) 204.
- [66] Q. Sun, J.-M. Jehng, H. Hu, R.G. Herman, I.E. Wachs and K. Klier, ACS Meeting, March 13–18, 1994, San Diego, CA.
- [67] J.M. Stencel, *Raman Spectroscopy for Catalysis*, Van Nostrand-Reinhold, New York, 1990.
- [68] M. Mehicic and J.G. Grasselli, in J.G. Grasselli and B.J. Bulkin (Editors), *Analytical Raman Spectroscopy*, Wiley, New York, 1991.
- [69] P.L. Villa, F. Trifiro and I. Pasquon, *React. Kinet. Catal. Lett.*, 1 (1974) 341.
- [70] F.R. Brown and L.E. Makovsky, *Appl. Spectrosc.*, 31 (1977) 44.
- [71] F.R. Brown, L.E. Makovsky and K.H. Rhee, *J. Catal.*, 50 (1977) 162.
- [72] F.R. Brown, L.E. Makovsky and K.H. Rhee, *J. Catal.*, 50 (1977) 385.
- [73] R. Thomas, J.A. Moulijn and F.P.J.M. Kerkhof, *Recl. Trav. Chim. Pays-Bas*, 96 (1977) M114.
- [74] S.L.K.F. de Vries and G.T. Pott, *Recl. Trav. Chim. Pays-Bas*, 96 (1977) M115.
- [75] F. Roozeboom, J. Medema and P.J. Gellings, *Z. Phys. Chem. (Frankfurt)*, 111 (1978) 215.
- [76] F.P.J.M. Kerkhof, J.A. Moulijn and R.J. Thomas, *J. Catal.*, 56 (1979) 279.
- [77] A. Iannibello, P.L. Villa and S. Marengo, *Gazz. Chem. Ital.*, 109 (1979) 521; A. Iannibello, S. Marengo, P. Tittarelli, G. Morelli and A. Zecchina, *J. Chem. Soc., Faraday Trans. 1*, 80 (1984) 2209.
- [78] J.-M. Jehng and I.E. Wachs, *Solid State Ionics*, 32/33 (1989) 904; ACS Div. Petrol. Chem. Preprints, 34(3) (1989) 546.
- [79] H. Knozinger and H. Jeziorowski, *J. Phys. Chem.*, 82 (1978) 2002; H. Jeziorowski and H. Knozinger, *J. Phys. Chem.*, 83 (1979) 1166.
- [80] H. Jeziorowski, H. Knozinger, P. Grange and P. Gajardo, *J. Phys. Chem.*, 84 (1980) 1825; H. Jeziorowski and H. Knozinger, *Appl. Surface Sci.*, 5 (1980) 335.
- [81] E. Payen, J. Barbillat, J. Grimblot and J.P. Bonnelle, *Spectrosc. Lett.*, 11 (1978) 997; P. Dufrense, E. Payan, J. Grimblot and J.P. Bonnelle, *J. Phys. Chem.*, 85 (1981) 2344; S. Kasztelan, J. Grimblot, J.P. Bonnelle, E. Payan, H. Toulhoat and Y. Jaquin, *Appl. Catal.*, 7 (1983) 91.
- [82] C.P. Cheng and G.L. Schrader, *J. Catal.*, 60 (1979) 276.
- [83] L. Wang and W.K. Hall, *J. Catal.*, 66 (1980) 276; 77 (1982) 232; 83 (1983) 242.
- [84] L. Wang and W.K. Hall, *J. Catal.*, 82 (1983) 177.
- [85] G.L. Schrader and C.P. Cheng, *J. Catal.*, 80 (1983) 369.

- [86] S.S. Chan, I.E. Wachs, L.L. Murrell, L. Wang and W.K. Hall, *J. Phys. Chem.*, 88 (1984) 5831.
- [87] J.M. Stencel, L.E. Makovsky, T.A. Sarkus, J. de Vries, R. Thomas and J. Moulijn, *J. Catal.*, 90 (1984) 314.
- [88] F.D. Hardcastle and I.E. Wachs, *J. Mol. Catal.*, 46 (1988) 173.
- [89] J.-M. Jehng and I.E. Wachs, *Catal. Today*, 8 (1990) 37; *J. Phys. Chem.*, 95 (1991) 7373.
- [90] J. Vedrine (Editor), *Catal. Today*, 20 (1994).
- [91] P.C. Mitchell and F. Trifiro, *J. Catal.*, 33 (1974) 350.
- [92] A. Zecchina, E. Garrone, G. Ghiotti and G. Minelli, *J. Phys. Chem.*, 79 (1975) 966.
- [93] R. Nakamura, F. Abe and E. Echigoya, *Chem. Lett., Jap. Chem. Soc.*, (1981) 51.
- [94] Y. Nakagawa, T. Ono, H. Miyata and Y. Kubokawa, *Chem. Soc., Faraday Trans. 1*, 79 (1983) 2929.
- [95] J. Sonnemans and P. Mars, *J. Catal.*, 31 (1973) 209.
- [96] F.E. Kiviat and L. Petrakis, *J. Phys. Chem.*, 77 (1973) 1232.
- [97] K. Segawa and W.K. Hall, *J. Catal.*, 77 (1982) 221.